



ELSEVIER

Nuclear Instruments and Methods in Physics Research B 172 (2000) 274–280

**NIM B**  
Beam Interactions  
with Materials & Atoms

www.elsevier.nl/locate/nimb

## Automated evaluation of $^{14}\text{C}$ AMS measurements

S. Puchegger\*, W. Rom, P. Steier

Vienna Environmental Research Accelerator, Institut für Isotopenforschung und Kernphysik der Universität Wien, Währinger Straße 17, A-1090 Vienna, Austria

### Abstract

The huge amount of raw data collected during routine  $^{14}\text{C}$  AMS measurements requires sophisticated processing tools to guarantee the quality and reliability of the resulting radiocarbon dates. This paper discusses the automatic evaluation system, that is in use and under continuous development at the Vienna Environmental Research Accelerator (VERA) laboratory. It includes a calibration program which is able to handle the bomb-peak. The flexibility of the system allows its use for other rare isotopes also. © 2000 Elsevier Science B.V. All rights reserved.

PACS: 29.85.+c

Keywords: Data evaluation; Filter; AMS; Radiocarbon

### 1. Introduction

Procedures for automated data evaluation have been used for many years at AMS laboratories (e.g. [1,2]). It is virtually impossible to ‘manually’ [3] evaluate all the data produced by an AMS system during a routine measurement: a measurement on a certain ‘sputter target’ – termed a ‘run’ – typically consists of 2000 ‘cycles’, each with a length of 100 ms. (The technical terms in this paper are innate to the VERA laboratory and may be different to those used at other facilities.) During each cycle, the three isotopes are injected sequentially into the accelerator by a switching high

voltage applied to the electrically insulated injector magnet chamber. The pulsed  $^{12}\text{C}$  and  $^{13}\text{C}$  currents, which are injected for 0.5 and 3 ms, respectively, are measured in Faraday cups, the radionuclide  $^{14}\text{C}$  is registered with a semiconductor detector in the remaining 96.5 ms of the cycle. For a complete measurement about 15 runs are performed on each of the 40 sputter targets. This takes about 40 h and amounts to several hundred megabytes of raw data.

Contrary to a manual evaluation, an automatic evaluation allows to check thousands of ASCII files for the occurrence of hardware and software problems and to do a more complex evaluation scheme. Since preliminary results are of interest from the very beginning of the measurement, an ‘on-line’ evaluation was one of the main goals. The system updates the results immediately after the completion of each run and supports the operator in assessing the status of the measurement.

\* Corresponding author. Tel.: +43-1-4277-51713; fax: +43-1-4277-9517.

E-mail address: stephan.puchegger@ap.univie.ac.at (S. Puchegger).

This paper presents a survey of automatic data analysis and evaluation methods used at VERA. A schematic layout of the facility can be found in [4].

## 2. Machine instabilities and other surprises

Hardly any measurement of a complete target wheel is void of instabilities and machine malfunctions. These influences may (e.g., unstable terminal voltage) or may not (e.g., eccentricity of the target wheel) be obvious in the results. In fact, most of the disturbances last for a very short time, influencing only a few cycles, which is not evident in the average value of the currents measured during a run. Therefore, a ‘per-cycle’ analysis is required.

The data evaluation system at the VERA laboratory consists of different stages that handle different types of known problems. Nevertheless, an experienced person is always needed to check for malfunctions that may have never turned up before.

### 2.1. The beam-current filter

The stability of the  $^{12}\text{C}$  and  $^{13}\text{C}$  currents is the main indicator for the short term stability of the machine, since the currents have rather small uncertainties and a high time resolution. Due to counting statistics, it is hardly possible to deduce such information from the  $^{14}\text{C}$  count-rate. The first step of the automatic evaluation is therefore the analysis of the high- and low-energy beam-currents.

The basic idea for the ‘peak filter’ is to compare each datapoint with one extrapolated from the preceding points by linear regression. Deviations from the extrapolated value, which exceed a certain level, indicate instabilities. In this case, neither the  $^{12}\text{C}$  and  $^{13}\text{C}$  currents nor the  $^{14}\text{C}$  counts may represent a sensible measure of the isotope ratio in the sputter target. Thus, the data collected during instabilities are excluded from the calculation of the mean values and of the respective isotopic ratios of the run. The limits for the filtering are selected by the operator and should be well above

the inherent measurement noise. Since the implementation of the automatic evaluation in early 1998, a large number of typical ‘patterns’ in the beam-currents have emerged, of which only some are characteristic for a specific problem (e.g., accelerator sparks, source sparks).

The second part of the filter system, the ‘slope filter’, tries to identify tendencies, which are missed by the peak filter, since they are visible only if a few hundred cycles are taken into account. Beside machine instabilities, most of these variations seem to originate in the sputter targets. Targets sputtered for the first time have a relatively high content of molecular ions, among them  $^{12}\text{CH}^+$ , which produce characteristic falling currents in the mass-13 low-energy Faraday cups. It is our standard procedure to remove these time intervals. Some cathodes show this kind of falling low-energy mass-13 current even after the first measuring run, in rare cases a target never yields a stable ion current.

To calculate the ‘steepness’ of the beam-current function, it is necessary to smooth the measurement noise with an ‘Optimal Wiener Filter’ [5]. A correct functioning of the slope filter requires that all spikes that exceed this noise are removed by the peak filter beforehand. The value of the maximum steepness accepted is up to the operator and highly subjective. The average currents for the remaining ‘good’ time intervals are calculated from the original unsmoothed datasets.

### 2.2. The wheel eccentricity correction

Our ion source is highly sensitive to the centering of the target wheel. A wheel eccentricity of only 15/1000 mm results in a shift of the beam-profile (measured at the exit of the electrostatic analyzer) of 3/10 mm for sputter targets at opposite wheel positions. Depending on the quality of the beam-tuning, this leads to deviations in the measured isotope ratios of up to 1%. Despite wheel re-adjustments that should center the wheel within an uncertainty of 5/1000 mm the eccentricity still seems to be a relevant reason for the remaining systematic uncertainties of up to 0.3% in our data.

Systematic investigations revealed that the eccentricity in the data can be handled by a sinusoidal correction without compromising the results, as long as the eccentricity is small.

$$X_{m\theta} = X_m \left( 1 + A \sin \left( 2\pi \frac{\theta}{40} \right) + B \cos \left( 2\pi \frac{\theta}{40} \right) \right), \quad (1)$$

where  $X_{m\theta}$  denotes the measured ratio,  $m$  the target material, and  $\theta$  is the target position in the wheel ( $0, \dots, 39$ ). To obtain the coefficients  $A$  and  $B$ , identical sputter targets are needed at (preferably) opposite positions in the target wheel. Usually we use at least two standard materials for this purpose. The corrected mean value of all targets of the same material is then

$$X_m \approx \frac{1}{\sum_{\theta} (1/\sigma_{m\theta}^2)} \sum_{\theta} \frac{1}{\sigma_{m\theta}^2} X_{m\theta} \times \left( 1 - A \sin \left( 2\pi \frac{\theta}{40} \right) - B \cos \left( 2\pi \frac{\theta}{40} \right) \right), \quad (2)$$

where  $\sigma_{m\theta}$  is the measurement uncertainty of material  $m$  at the position  $\theta$ . Minimizing

$$\sum_{m\theta} \frac{(X_{m\theta} - X_m)^2}{\sigma_{m\theta}^2} \quad (3)$$

will then give values for  $A$  and  $B$ . The uncertainty of  $A$  and  $B$  is estimated by Gaussian error propagation of the  $\sigma_{m\theta}$ . This calculation is done separately for both  $^{14}\text{C}/^{12}\text{C}$  and  $^{13}\text{C}/^{12}\text{C}$  ratios (see Fig. 1).

Since we are aware that this correction is disputable, we usually stop the measurement once a significant eccentricity is visible and repeat the tuning of the machine. Up to now, this always solved the problem. However, the already measured data are corrected.

Recently, we succeeded in compensating the eccentricity of the target wheel by automatically adjusting the first steering elements after the source (horizontal ESA and vertical steerer plates) for each target individually. Their setting is varied by our automatic tuning algorithm [6] to achieve maximum transmission through the accelerator. The eccentricity of the target wheel is then

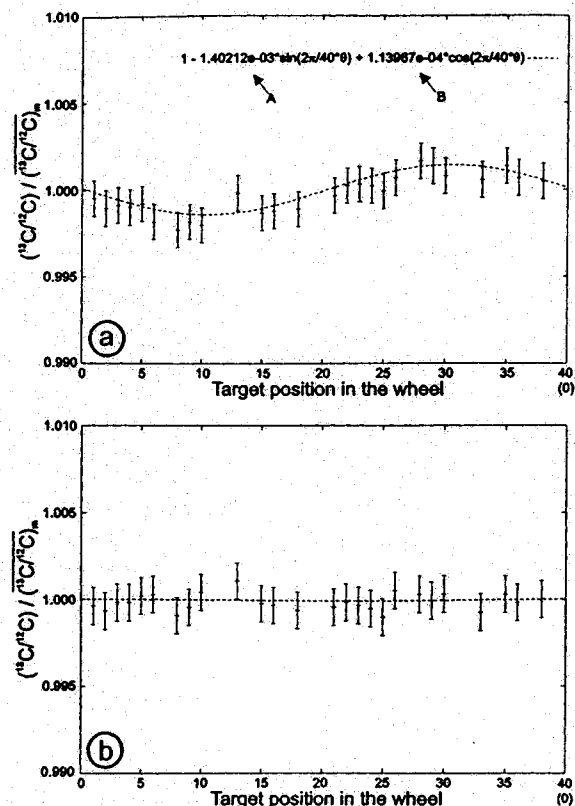


Fig. 1. The eccentricity correction of a standard  $^{14}\text{C}$  measurement. The data are plotted as  $^{13}\text{C}/^{12}\text{C}$  ratio on a certain target divided by the mean ( $m$ ) of that ratio for all identical targets (usually two at opposite positions in the wheel). Graph (a) is the data previous to correction. The broken line is the best sinusoidal fit (see text). Graph (b) shows the data after correction.

reflected in the values found for the steering elements, but is no longer visible in the measured isotopic ratios. A mechanical solution of the eccentricity by a modified wheel mounting may also be possible (private communication by NEC).

### 3. Quality control

On the one hand, a meaningful quality control system should be able to monitor the acquired data for known problems, and on the other hand, it should offer the flexibility to extend the quality control to new parameters whenever a new kind of disturbance shows up.

The beam-current filter algorithms cope only with a single run and therefore cannot detect long-term tendencies, which extend over several turns of the target wheel. We strive to uncover such tendencies with various quality control tests (e.g., the slow but steady increase of the stripper gas pressure because of a malfunctioning valve).

Our quality control system assigns two marks to each run. These marks describe the individual performance of the run and the agreement with the other runs on the same sputter target, respectively, using the formula

$$\sum_i \left( \frac{|X_i - Y_i|}{\Delta_i} \right)^{p_i}, \quad (4)$$

where  $X_i$  can be any logged machine parameter or any value calculated by the run evaluation,  $Y_i$  a reference value assigned by the operator, and  $\Delta_i$  is the deviation resulting in a mark of 1.0. We hope that the  $p_i$  provides enough flexibility for all our future needs. Tests for an arbitrary number of parameters are possible and the results are added up.

### 3.1. The quality mark

The mark measuring the performance of a single run is compared with a given value (usually 1.0), above which the run is excluded from the further evaluation. A good example for such a test is the 'cycle yield' (see Fig. 2), i.e., the percentage of all cycles of a run that have not been removed by the beam-current filter described before. The usual selection of  $\Delta$  and  $p$  is such that every run with a cycle yield of less than 80% is removed.

### 3.2. The continuity mark

A second mark measures how well the isotope ratio from a certain run agrees with the previously measured data. This is achieved by defining  $X_i$  as the isotope ratio from the actual run,  $\Delta_i$  as its uncertainty and  $Y_i$  as the average of all previous runs on the same sputter target. This mark is not used to exclude any data from the evaluation, but it proved to be a highly sensitive quality control

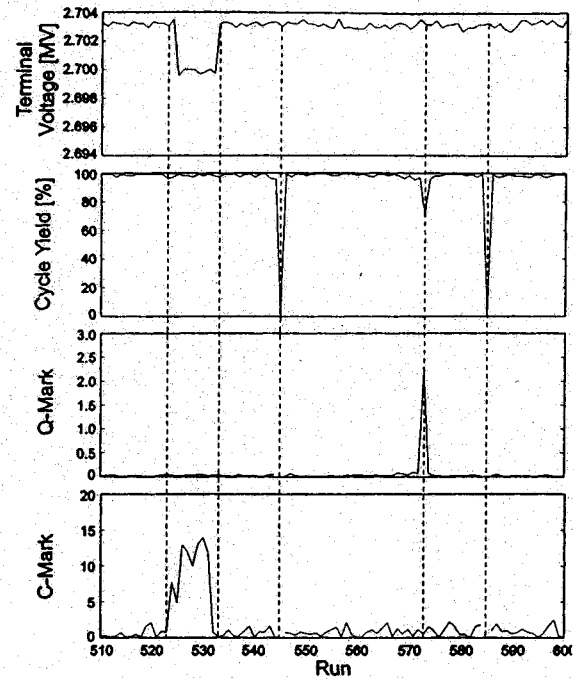


Fig. 2. Quality control of a standard  $^{14}\text{C}$  measurement. The shift in the terminal voltage (which originated in a programming error) does not necessarily produce a deviation, which is noticed by the filter system. Only the measured isotope ratios differ from previous measurements on the same target, which results in an increased continuity mark (C-Mark). The measurements with a cycle yield well below 100% either have an increased quality mark (Q-Mark), or were eliminated from the evaluation before the quality control already if the cycle yield is 0% (runs 545 and 585).

parameter to detect malfunctions, where no specialized tests yet exist.

## 4. On-line and off-line evaluation

One of our main goals was to create an operating system independent access to the data evaluation. Since both the accelerator control computer and the evaluation server are Linux machines, and all workplace computers are equipped with Windows NT, we felt that a WWW-based approach would suit our needs best.

The basic evaluation software is implemented as command-line driven C programs, which read and write plain ASCII files. A 'bash' shell-script

coordinates the execution. So-called 'CGI' scripts reformat the data from plain ASCII files to (hopefully) comprehensible HTML documents on demand, when accessed by the user through the www browser at his PC. The HTML interface also includes data visualisation routines that have been written in Java for maximum flexibility.

The on-line evaluation system updates the results as soon as a new run is finished. Every authorized user can then create independent off-line 'evaluations', i.e., different versions of the evaluation which do not interfere with each other. All evaluation parameters are stored in a file which can be modified through HTML forms before triggering a (re-)evaluation. For a 40-h measurement, a complete re-evaluation takes about 20 min. The last step is to select one evaluation as the final one. Although it is advantageous to have data acquisition/evaluation and quality control done by different persons, this is not always possible due to a shortage of experienced staff.

#### 4.1. (On-line) radiocarbon calibration

None of the commonly available calibration programs can easily be integrated into our evaluation system, since they lack a command-line driven interface. Moreover, a forensic case triggered interest in the dating of recent samples [7]. For this, we had to extend the calibration curve published in [8] with atmospheric data by Levin [9], since no calibration curve available at that time did include the bomb-peak. Our standard calibration program OxCal 2.18 [10] could not cope with the initial steepness of the bomb-peak. So we decided to develop our own calibration tool. The fully tested source code [11] is written in C++ and can be used as a stand-alone tool.

The algorithm used in the program to interpolate the calibration curve produces a resultant curve, that is free of unnatural wiggles [12]. The common procedure of probabilistic calibration programs is to step along the calibrated age axis with a fixed stepsize (usually a one-year interval). A problem arises, because the probability is sampled in the center of the intervals only. Steep changes in the calibration curve, as in the bomb-peak time, then lead to a failure of the numeric

algorithm. The sampling will very likely 'step over' the centerpiece of the probability distribution on the radiocarbon axis. The thin peaks on the calibrated age axis, originating in the steep calibration curve, are then not adequately reproduced by the numerical algorithm and erroneously excluded from the confidence intervals.

There are two mathematically equivalent solutions to overcome this problem (see Fig. 3):

- It is possible to adapt the stepsize on the calibrated age axis to the steepness of the calibration curve.
- The straightforward solution, that we chose to implement, is to use evenly spaced steps on the radiocarbon age axis corresponding to a varying interval length on the calibrated age axis. This procedure accurately yields the twofold solution for the descend and the ascend of the bomb-peak.

The new approach produces a larger stepsize in flat regions of the calibration curve than the usual approach. However, this has negligible influence on the result.

## 5. Summary

The automatic data evaluation system not only saved a lot of time compared to the 'manual' evaluation before, but also improved confidence in the results. It allows complex evaluation schemes to be applied routinely before the measurement has been finished. The use of different independent evaluation versions makes it easy to study the influence of certain evaluation parameters on the final results.

The operator now checks the eccentricity coefficients and the diagnostic marks every few hours. In a recent extension, the automatic evaluation software may pause the measurement if no usable data are acquired for a certain time.

A new calibration tool has proven its usefulness in forensic investigations (bomb-peak dating) and will be integrated into the automatic evaluation system. In regions previous to the bomb-peak, the results are similar to common calibration programs.

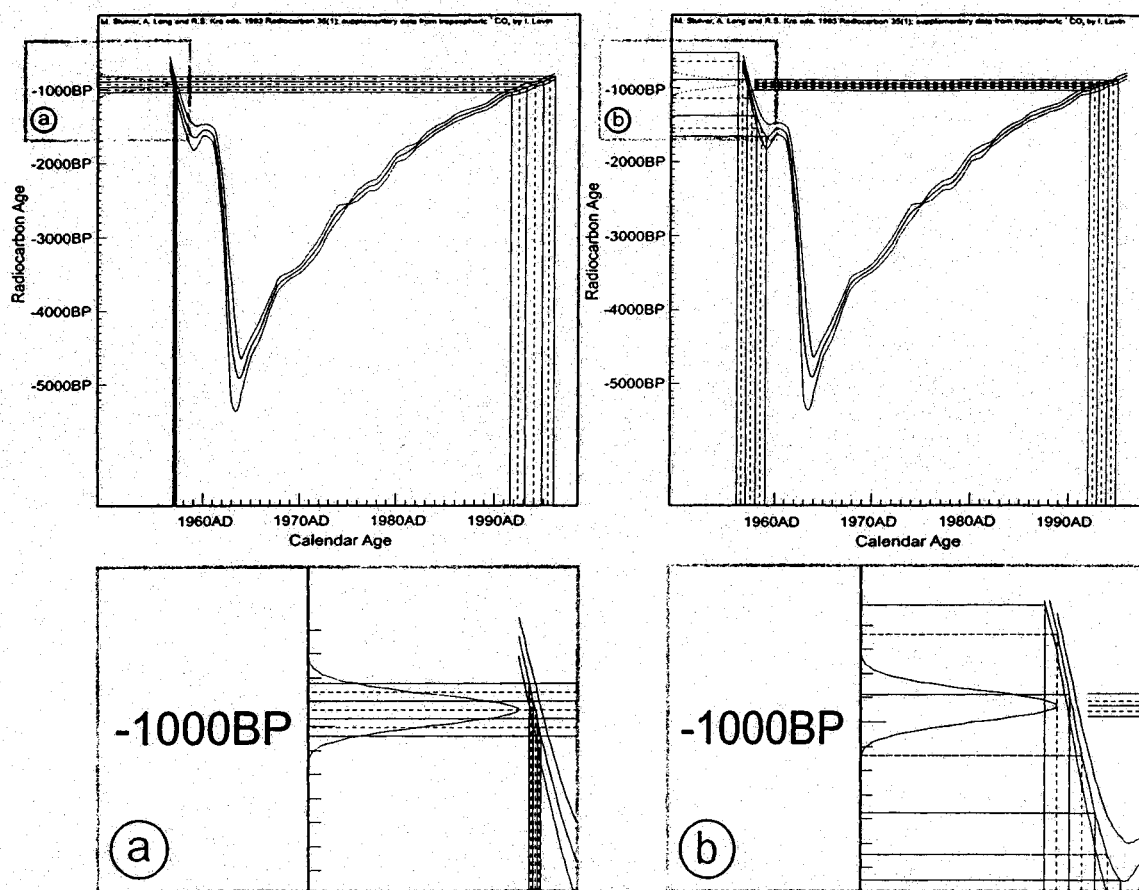


Fig. 3. A comparison of the two approaches to calibration in the bomb-peak time. The integration intervals in the figure have been chosen much larger than in real applications to illustrate the two different approaches. (Please note that these intervals are not chosen according to confidence limits.) The left side shows the new approach with an equal spacing on the radiocarbon age axis, whereas the right side displays the conventional approach with an equal spacing on the calibrated age axis. The probability distribution on the calibrated age axis in the bomb-peak era usually consists of two main regions. The new approach produces a very narrow interval spacing (closeup (a)) on the calibrated age axis for the steep slopes and thus approximates well the 'true' probability distribution. The commonly used equal spacing on the calibrated age axis will not adequately reproduce the narrow peaks, unless the stepsize is chosen extremely small (many intervals per year). The dashed lines indicate the centers of the intervals, where the value for the integration is sampled. Closeup (b) shows a case where the sampling points of the intervals miss the main part of the probability distribution on the radiocarbon age axis (dotted curve).

## References

- [1] F.H. Séguin, R.J. Schneider, G.A. Jones, K.F. von Reden, Nucl. Instr. and Meth. B 92 (1994) 176.
- [2] R.J. Schneider, G.A. Jones, A.P. McNichol, K.F. von Reden, K.L. Elder, K. Huang, E.D. Kessel, Nucl. Instr. and Meth. B 92 (1994) 172.
- [3] A. Priller, R. Golser, P. Hille, W. Kutschera, W. Rom, P. Steier, A. Wallner, E. Wild, Nucl. Instr. and Meth. B 123 (1997) 193.
- [4] A. Priller, T. Brandl, R. Golser, W. Kutschera, S. Puchegger, W. Rom, P. Steier, C. Vockenhuber, A. Wallner, E. Wild, Nucl. Instr. and Meth. B 172 (2000) 100.
- [5] W.H. Press, Saul A. Teukolsky, William T. Vetterling, Brian P. Flannery, Numerical Recipes in C, second ed., Cambridge University Press, London, 1992, p. 994.
- [6] P. Steier, S. Puchegger, R. Golser, W. Kutschera, A. Priller, W. Rom, A. Wallner, E. Wild, Nucl. Instr. and Meth. B 161–163 (2000) 250.

- [7] E. Wild, U.K.A. Arlamovky, R. Golser, W. Kutschera, A. Priller, S. Puchegger, W. Rom, P. Steier, W. Vycudilik, *Nucl. Instr. and Meth. B* 172 (2000) 944.
- [8] M. Stuiver, A. Long, R.S. Kra (Eds.), *Radiocarbon* 35 (1) (1993) 244.
- [9] I. Levin, B. Kromer, *Radiocarbon* 39 (2) (1997) 205.
- [10] C. Bronk Ramsey, *Radiocarbon* 37 (2) (1995) 425.
- [11] S. Puchegger, Calibrate home page: <http://www.univie.ac.at/kernphysik/puchegger/calibrate> (2000).
- [12] H. Akima, *J. Assoc. Comput. Mach.* 17 (1) (1970) 589.